Calibration Report of

the PEACE Measurements

in the Cluster Active Archive (CAA)

prepared by

A.N. Fazakerley, N. Doss, A.D. Lahiff,
I. Rozum, D. Kataria, H. Bacai, C. Anekallu, B. Mihaljčić,
G.Watson, M. West and A. Åsnes

1 Introduction

The Plasma Electron and Current Experiment (PEACE) instruments, working on each of the four Cluster spacecraft, measure 3D electron velocity distributions during each spacecraft spin. Moments of these distributions, and pitch angle data are also produced.

This document provides a brief description of the PEACE instruments, information about how the calibration parameters are assessed, and an indication of the calibration quality that has been achieved through calibration and cross-calibration work. A significant part of the material included here is also presented in a paper on Cluster-PEACE In-flight Calibration status prepared for the Proceedings of the Cluster Workshop and CAA School (Fazakerley et al., 2010a) and in a published paper titled In-flight calibration of the Cluster PEACE sensors (N. Doss et al., 2014).

2 Instrument Description

Each Cluster spacecraft carries an identical PEACE instrument, consisting of two sensors, HEEA (High Energy Electron Analyser) and LEEA (Low Energy Electron Analyser), and a data processing unit, the DPU. The instruments are described in Johnstone et al (1997), Fazakerley et al. (2010b) and the CAA PEACE ICD (Fazakerley et al., 2008).

The measurement principle of each analyser is illustrated in Figure 1. The arrangement of the HEEA and LEEA sensors on a spacecraft, and the anode numbering, is illustrated in Figure 2. The spacecraft generally oriented with the spacecraft spin axis pointing close to the negative Z direction in GSE coordinates.

The LEEA is designed to cover the lowest electron energies (< 10 eV) but is also capable of covering the full energy range up to ~26 keV. LEEA has a geometric factor appropriate for the higher electron fluxes usually found at lower energies (e.g., in the solar wind and magnetosheath). The HEEA has a larger geometric factor, better suited to the outer magnetosphere, which extends the dynamic range of the instrument. Each sensor usually covers about 70% of the instrument energy range, and the sensors are used together to cover the full range every spacecraft spin.
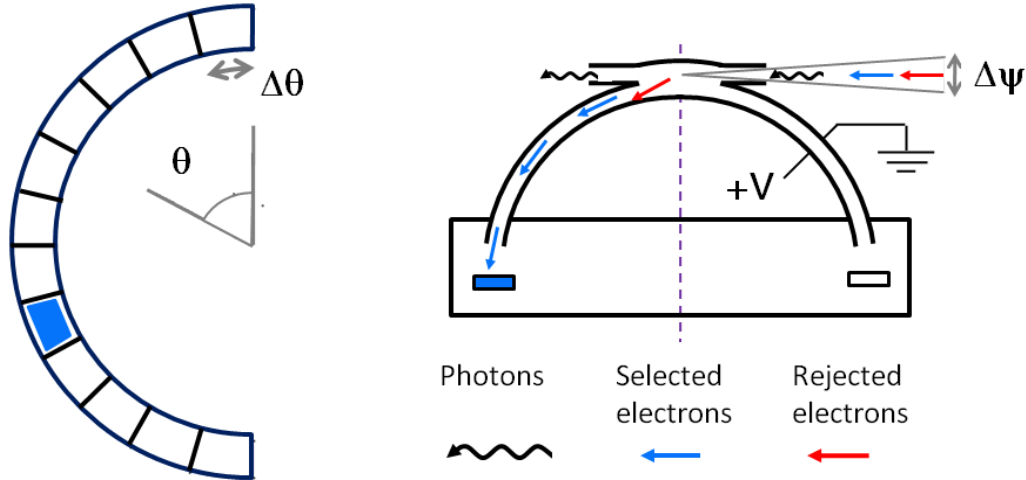
Fig. 1. Illustration of the principle of the PEACE Top Hat electrostatic analyser. The voltage applied to the analyser hemispheres diverts electrons (shown in blue) of a specific narrow band of energy and arriving within the acceptance angle $\Delta\Psi$ through the analyser to the detector, while electrons of other energies (e.g., in red) strike one of the analyser hemispheres and are not detected. The semi-annular MCP amplifies the signal of an electron reaching it, and the resulting charge cloud is detected by one of 12 segments of the anode beneath, giving information about the electron arrival direction θ. The Top Hat design is able to provide a focussed spot in the detector plane for a parallel electron beam arriving from anywhere in the aperture plane. At times when the aperture looks sunward, the majority of photons (black wiggly arrow) pass through the aperture and do not find their way to the detector.

3 Measurement Calibration Procedures

The major uncertainty of instrument calibration is the MCP detection efficiency, or sensitivity, which varies with time, and which can vary differently on different parts of the semi-annular MCP. Calibration parameters which are associated with the physical structure of each analyser, such as the geometric factor and the k-factor, are stable and well established. The PEACE calibration parameters are outlined in Appendix A. The ground calibration work established values for most of the important, non-time varying parameters for each individual sensor before launch.

In-flight calibration is required to keep track of (and provide corrections for) changing MCP detector efficiency, represented by

$$\varepsilon_{ik} = \alpha\varepsilon_0 \, \beta_{ik}\varepsilon(v_k^2)_i \, \gamma_{ijk}$$

where :

- ε_0 is constant by definition, and for the determination of this value, please see section 6.1
- α is a time dependent correction factor for ε_0 (absolute detector efficiency), used to describe the effect of sub-optimal detector efficiency. In work to date, we have made the assumption that this factor applies equally for all anodes (may in fact be incorrect).
- β_{ik} represents corrections for each anode to $\varepsilon(v_k^2)_i$, the relative sensitivity of individual 12 anodes of each detector, which may in principle vary with energy. Experience shows that these correction factors also depend on α.
- γ_{ijk} represents possible under-counting due to detector saturation in high flux environments (not to be confused with electronic dead time, which sets in at higher count rates). This is not usually a problem for LEEA, nor for HEEA except during time intervals of especially high fluxes in environments like the magnetosheath.

The time history of these parameters is determined from PEACE data, as discussed in Section 5.

In-flight calibration was also required to refine knowledge of ε_0. This has been achieved through cross-calibration of electron density measurements with the WHISPER experiment, using data from the early years of the mission, as discussed in Section 6.
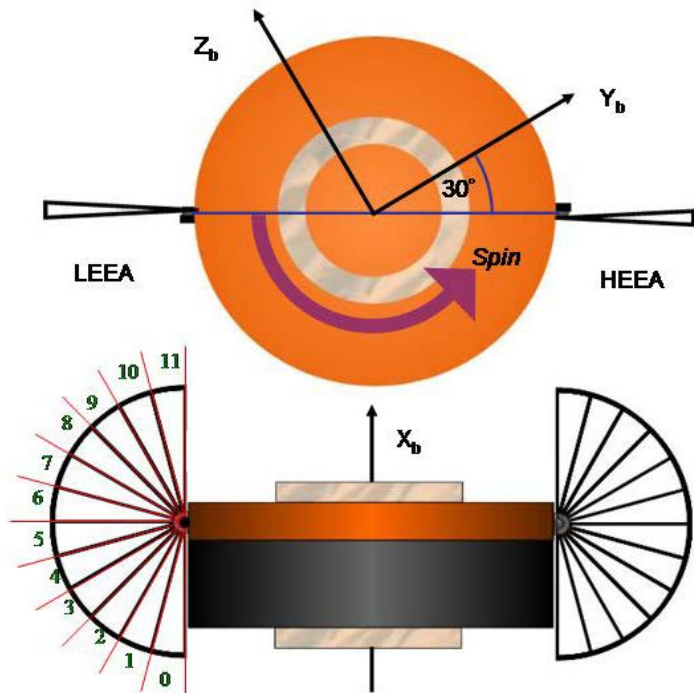

Fig. 2. The physical deployment of the sensors on the spacecraft. The spacecraft body coordinate system is shown (Xb, Yb, Zb). The sensor numbering with respect to the spin axis is indicated, e.g., zone 0 looks towards –Xb, and sees electrons with velocities along the spin axis direction, +Xb. In orbit the spacecraft spin axes are maintained roughly anti-parallel to the GSE Z axis.

The PEACE data can be based on the following calibration procedures. The following calibration versions can be found in the PEACE CAA files, and v5.1 is also mentioned as examples produced with this calibration are shown later in the report (e.g. section 6.4):

Version	Alpha	Inter-anode	Calibration procedure details	Validity details
v5.1	yes	yes	Alpha factors derived using weekly MCP test method (see section 5.1) Inter-anode calibration included (see section 5.2)	C1, C2 (L&H) Jan 2001-May 2007 C3, C4 (H) Jan 2001-May 2007 C3 (L) Jan 2001-10 Apr 2007 C4 (L) Jan 2001-16 May 2006
v5.2	yes	yes	As V5.1 but produced with minor corrections to calibration codes, mainly expected to improve measurements of electron bulk velocity in the solar wind	*Used to produce 2001-2007 PEACE CAA data* **note that this interval is longer than the calibration validity dates for C3 and C4 LEEA*
v6.0	yes	no	Alpha factors derived using density comparisons with WHISPER (see Appendix B).	*Used to produce 2008 – 2015 PEACE CAA data*
v5.9	yes	no	Alpha factors were initially based on the v6.0 calibration from the last day in 2008*, taking into account MCP level variations.	*No longer applicable. Previously used to produce 2009 PEACE CAA data only, but all PEACE 2009 data was redelivered in 2016 with v6.0*
v6.1	yes	yes	Will consist of v6.0 alpha factors plus inter-anode calibrations	Will be available in the future PEACE CAA data for years 2005 onwards will be remade with this calibration when ready.

Table 1: Definition of PEACE calibration versions

Earlier calibrations versions exist but are not in PEACE CAA files. These begin with V1, based on ground calibration work, and develop to V5 as the techniques discussed below were developed.

4 Measurement Processing Procedures

The conversion of telemetered count rate data to data in scientific units follows a straightforward, conventional procedure. The key aspects are outlined in the Appendix A.

Background noise levels in the sensor have been quantified and are generally low. No attempt has been made to remove them in the data delivered to CAA thus far. A dual-sensor technique for removing background counts due to penetrating radiation has been developed for use during perigee passes through the magnetosphere's radiation belts or for data collected during Solar Proton Events, but it is not in routine use and at the time of writing the CAA dataset does not benefit from this procedure.

5 Results of Calibration Activities

5.1 Determination of α correction factors

Weekly tests of PEACE sensor performance are routinely carried out in order to produce a detailed time history of sensitivity variations for calibration purposes. These tests are performed by setting both sensors to observe the same energy range, and then varying the MCP voltage on one sensor while keeping the other sensor at normal operating voltage. The process is then repeated with the roles of the sensors exchanged. The response of the measured count rate to increasing voltage in the test sensor can be separated from count rate changes due to variations in the plasma environment using data from the second sensor. The principle and the practical implementation are illustrated in Figures 3-5. Figure 4 shows test results from 2003 and 2009 for one of the sensors, and show the effects of detector sensitivity decline over time, since a higher MCP voltage is needed to achieve an α approaching 1. The result is a detector sensitivity time history which we represent in terms of the α correction factor term: see for example Figure 6. Progressive extension of the α factor history is an ongoing task while mission operations continue.

At the time of writing, this method has ceased to be effective. The trend for the "S-curve" to move to higher MCP levels, as shown in Figure 4, has developed so that it is no longer possible to get a

full S-curve of the kind shown in Figure 4. An alternative approach based on density comparisons with WHISPER is now used routinely for all sensors – see Appendix B for update.
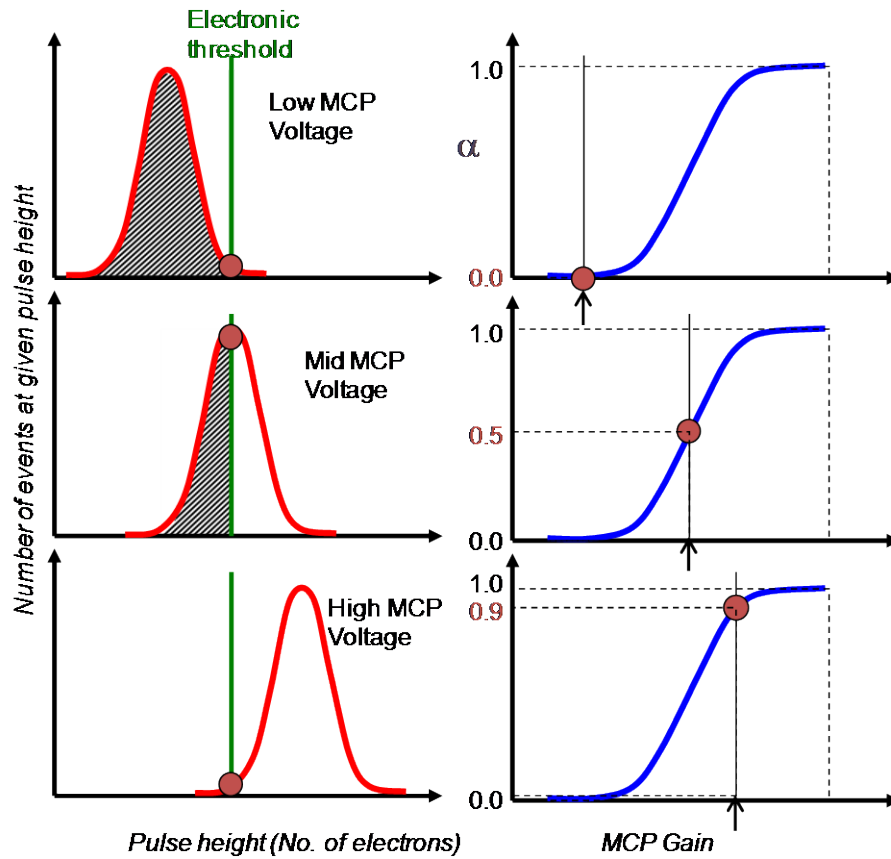

Fig. 3. Illustration of the principle of derivation of the α factor. The left-hand column shows the pulse height distribution in red, i.e. the spread of values of measured charge produced by the MCP in response to a large number of incident particles, for three possible values of the voltage applied across the MCP. The green line marks a threshold value of charge, below which the counter electronics ignore the signal. As the voltage across the MCP is increased, larger signals are generated and the pulse height distribution moves to the right, so that the fraction of the pulse height distribution above the threshold increases (white area under red curve in plots on the left-hand column). This fraction is the α factor which is ideally 1 so that all arriving electrons would generate a signal above the threshold and so be counted. The practical implementation is illustrated and described in Figure 5 and its caption.
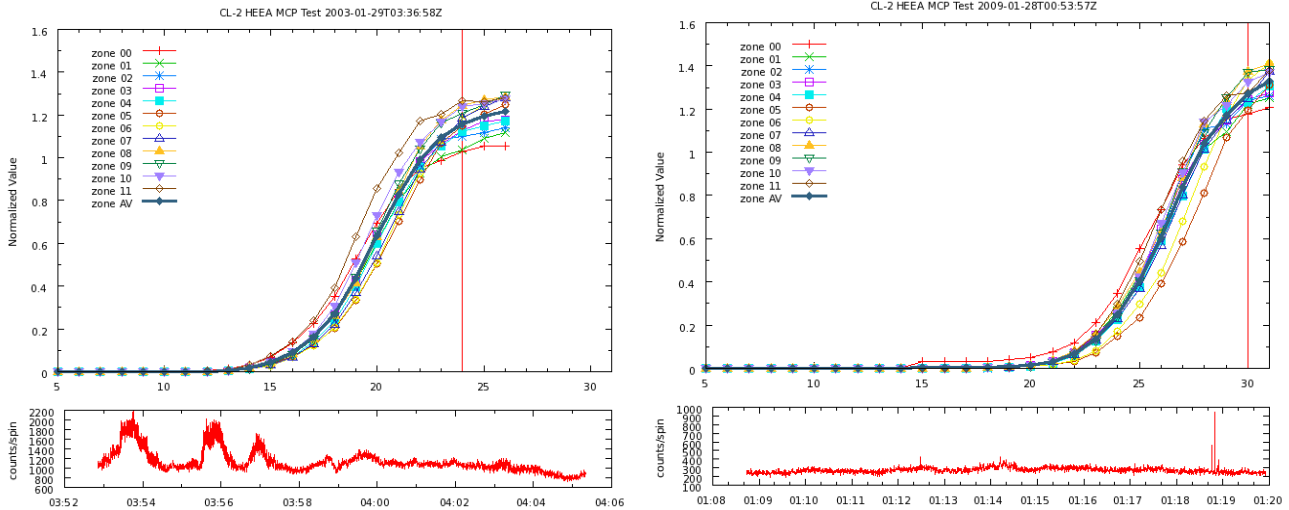
Fig. 4. Typical weekly MCP test results for the Cluster 2 HEEA sensor. The plots show data from 2003 (left) and 2009 (right) illustrating that the MCP voltage required to achieve a certain sensitivity has been raised as the mission proceeds – due to declining MCP performance over time. During a test, measurements are made over a range of HEEA MCP voltages, including the normal HEEA operating level, while simultaneous measurements by LEEA (operating at its normal operating voltage) provide information about changes in ambient plasma fluxes. The upper panels show the counts from the HEEA sensor after normalization using the LEEA sensor, as a function of voltage level. Curves are provided for each anode, together with the average (thick, dark line). The normalization includes a factor relating to the ratio of the nominal HEEA and LEEA geometric factors. The vertical red line shows the HEEA MCP voltage during normal operations as the time of the test. The lower panels show the number of counts detected by the LEEA sensor, which is monitoring the environment. Note that the ambient plasma fluxes are varying strongly in the 2003 case, showing the importance of using LEEA to normalize the data. MCP voltage level is converted to MCP gain using a ground-calibration dataset, using the assumption that the gain is known (= the counter electronic threshold) at the point of inflection of the S-curve, where $\alpha = 0.5$. Hence one may determine the MCP gain at the operational voltage or any other level at the time of the test.

Fig. 5. The counts ratios from a large number of MCP tests are plotted here; both HEEA/LEEA and LEEA/HEEA; after the ratios have been normalized so that the ratio is 1 at high MCP gains. The red line indicates the counter electronic threshold. The pale blue curve is the α factor expected if the pulse height distribution (PHD) is a simple Gaussian as illustrated in Fig.3. In practice the PHD appears to have a different form at low MCP gains, as the measured performance doesn't follow the model curve there, indicating that the true pulse height distribution is not Gaussian at low MCP gain (this is not unexpected, based on ground tests) We use an empirical fit to the data as the basis for our α vs. gain calibration.
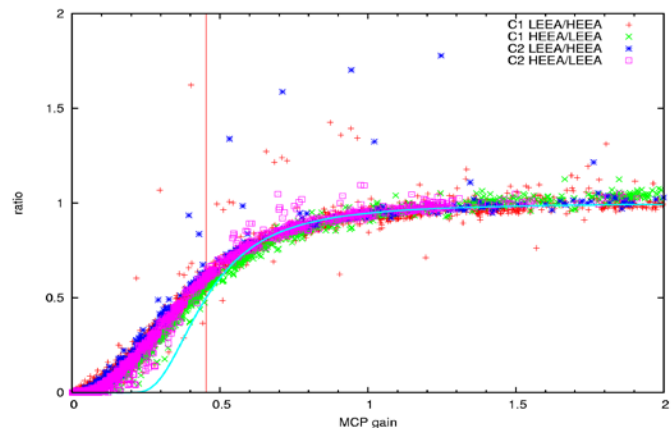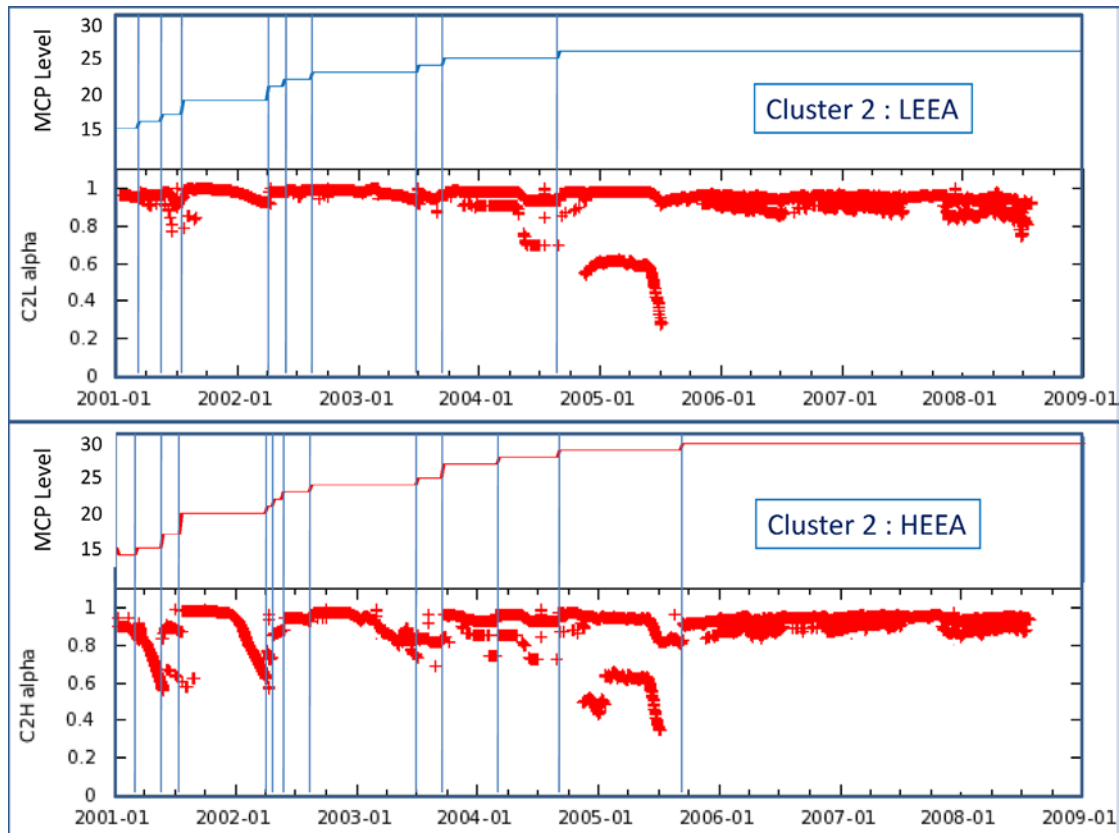
Fig. 6. The plot shows the time history of the α-factor for the Cluster 2 HEEA (below) and LEEA (above) sensors, together with the time history of the MCP levels used in normal operations (a proxy for the voltages across the MCPs). The main point to note is that the alpha factor which is ideally ~1 has been held near 1 in the later years, but in the early years of the mission it tended to decline in the early part of each year, especially for HEEA, until the MCP level was raised. The sensitivity decline was associated with prolonged exposure to high fluxes in the magnetosheath and solar wind. The exposure to high fluxes has been limited in the later phase of the mission either by deactivating the sensor in such regions (according to a duty cycle) or by operating the sensors with lowered MCP voltages in those regions. The lowered MCP levels are not shown on the MCP level plots (upper panels), but their consequences (two sets of crosses per day) are apparent in the α-factor plots, especially in early 2005. On such days, the lower alpha factor is applied when the MCP levels have been lowered and the upper value when the MCP levels are at normal operational level. The curves for other sensors (not shown) exhibit similar features, though in some cases (particularly Cluster 3 and 4) the α-factor values are not always so close to 1 later in the mission.

5.2 Determination of β correction factors

Our approach to estimating inter-anode relative sensitivity corrections is based on the requirement that when measuring gyrotropic pitch angle distributions which are varying only on long timescales, the same pitch angle may be observed by more than one anode for a sensor on a spinning spacecraft, and all such anodes should provide the same measured values of fluxes (in scien-

tific units) at that given pitch angle. The principle may be applied across the full pitch angle range. This general type of approach is also used for the CIS-CODIF sensors (see for example McFadden et al., 2007). In our approach, pitch angle data is fitted using a parabolic function, which may be used for isotropic plasma, and also for symmetrical departures from isotropy such as those with greater fluxes near 90° pitch angle, or enhanced bi-directional magnetic field aligned fluxes, as illustrated in Figure 7.

Fig. 7. An illustration of the process of fine-tuning inter-anode calibration. The chart shows data from preselected intervals, in units of differential energy flux versus pitch angle, for a collection of measurements in a single energy bin from a particular sensor. The blue curve is a parabola fitted to the data. The correction factors are those that are used to adjust the fluxes in individual anodes to fit the parabola as well as possible. The colours of the data points indicate which pair of anodes the data belongs to. Note that data from a given anode pair is often found over a spread of pitch angle values.
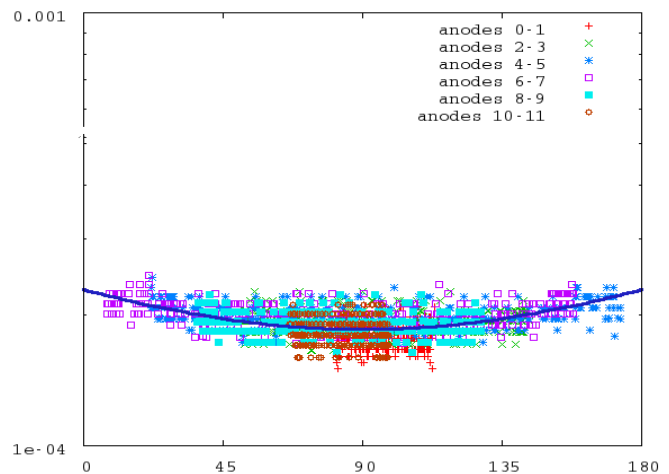
We have applied this principle in a large scale automated approach, testing each measured energy at which the count rate was considered acceptable, for all spins of data from data intervals where the plasma was selected to be relatively steady and with suitable temperature anisotropy. Temperature anisotropy values in the range $0.95 < T_{||} / T_{\perp} < 5$ (but commonly near 1) were used, provided the anisotropy values remained steady to within ±0.05 during chosen intervals; such intervals ranged in duration from 20 s to 360 s. The data selection process also rejected bad data intervals and cases with noise due to energetic particles in the radiation belts or solar energetic protons. The study focused on 3D data products in which the anode data is treated in anode-pairs, 3DR and 3DXP data (for details, see the PEACE UG). The main aim of the inter-anode calibration is to support generation of high quality velocity and higher order moments; thus we focus on 3DR and 3DXP as they comprise the majority of the 3D data and in particular as they are the data from which ground moments are usually calculated. During the period 2001-2004, between 100,000 and 200,000 individual intervals were used for each of the 8 PEACE sensors. The resulting correction factors β_{ik} were initially organized by energy and anode-pair. However, moments data produced using these calibrations were not very satisfactory. It was then recognized that

the correction factors β also showed a dependence on α, as illustrated in Figure 8. Therefore, by applying the appropriate correction factors for a given anode, energy and α (itself a function of time), the corrected calibrations could be used to produce moments which showed much improved accuracy. Although in principle the β factors can be determined for a given sensor and known α factor for time intervals not covered by the original study, work continues to extend the calibration correction factors dataset, as new data is provided by continuing mission operations.
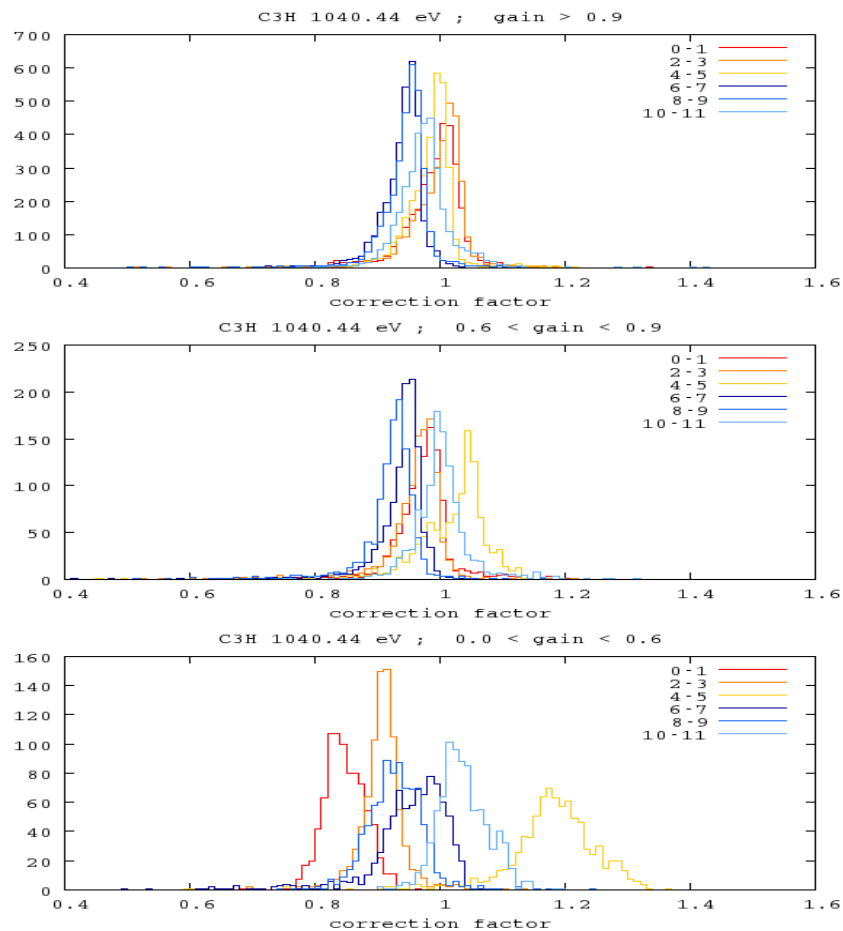

Fig. 8. The inter-anode correction factors for C3 HEEA. The three panels correspond to different MCP gain, with high gain (good performance) at the top, and lower gain in the lower panels. The plots show the distribution of inferred correction factors for each anode-pair, vs correction factor. It is apparent that as the gain departs increasingly from high values, the correction factors for different anodes diverge away from 1, indicating that measurement errors will be more severe at lower gains if uncorrected. Conversely, the appropriate correction factors can only be applied once the gain (via the α factor) has been assessed.

We validate this method by examining the statistics of $v\perp_z$ values determined using our improved calibrations (compare Figures 9 and 10). It is important to note that the method of determining correction factors does not make use of moments and in particular does not seek to minimize the average value of $v\perp_z$.

It has been suggested that an alternative approach which in essence derives a factor for each anode pair, thereby simultaneously dealing with gain dependent inter-anode calibration changes, but this has not been attempted to date. An attempt has been made to develop similar inter-anode calibration factors for each individual anode, which would be useful for pitch angle data, but this is currently on hold.
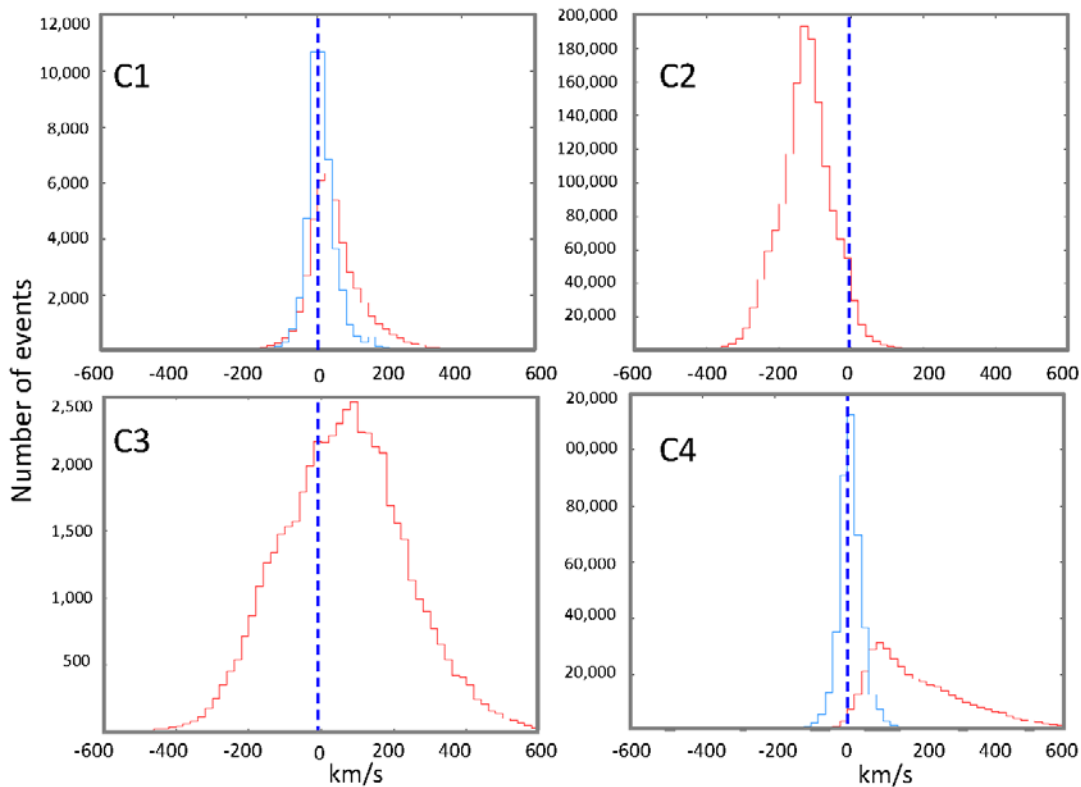

Fig. 9. Illustration of the quality of spin-axis components of $v\perp$, from PEACE-HEEA (red) and CIS-CODIF (blue) for a set of 208 magnetotail plasmasheet intervals during 2001-2003 BEFORE improvement of PEACE inter-anode relative calibrations, β. The plots use moments calculated from 3D data collected by the HEEA sensors.
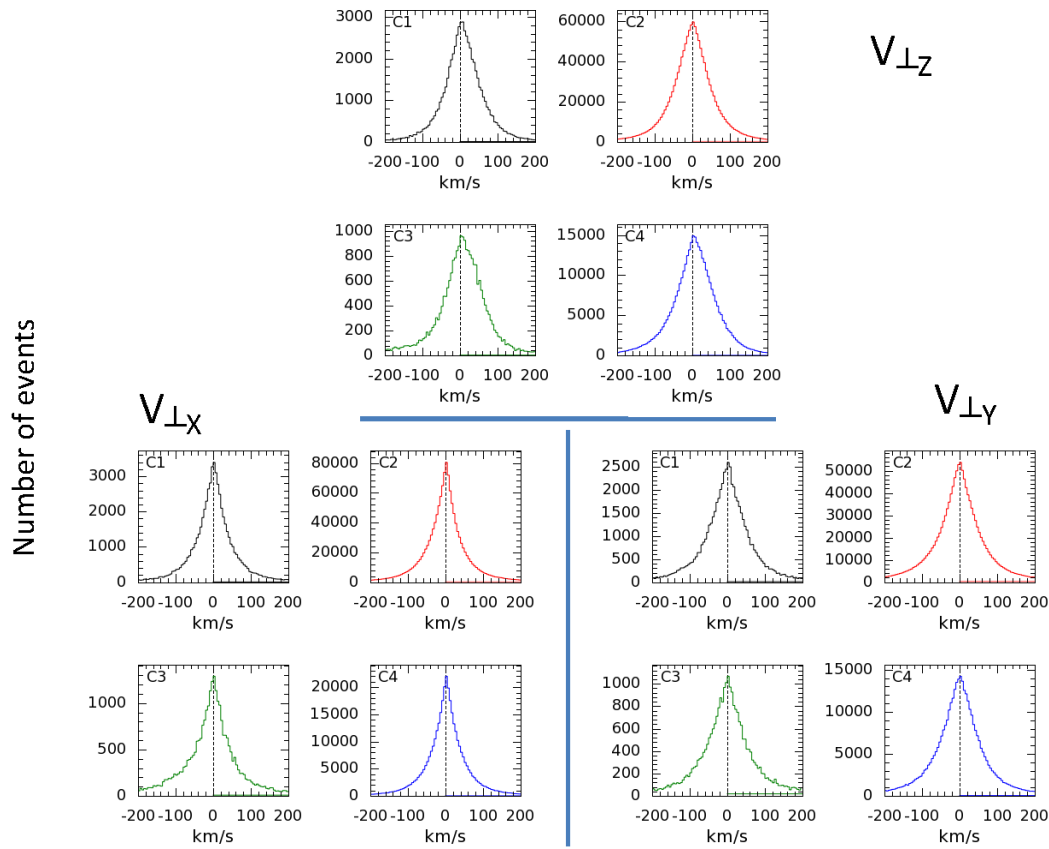
Fig. 10. Illustration of the quality of spin-axis components of PEACE-HEEA v⊥, for a set of plasmasheet intervals from 2001-2007 on spacecraft C1, C2 and C4, and 2001-5 on C3, AFTER improvement of inter-anode relative calibrations.

5.3 Determination of γ correction factors

No work has been carried out to attempt to correct for gain depression at high fluxes. This is likely to affect only the peak flux part of a measured distribution, so that any attempt to make a correction to the distributions may need to be implemented on a spin-by-spin basis and it could be rather complicated.

Work is ongoing to find a method of tagging time intervals where gain depression is occurring (i.e., where γ <1) however this is made more complicated because of underlying gain variations of the kind which are tracked using the α correction factor. The intention at this stage is to provide information in CAA data files to alert the user when gain depression due to high fluxes is thought to be affecting a sensor.

6 Results of Cross-Calibration Activities

6.1 PEACE-WHISPER Cross-calibration: Determination of ε_0 calibration parameter

The absolute detector efficiency ε_0 was determined using comparisons of density measurements between PEACE and the plasma wave instrument WHISPER. Only when the α history is available, together with $\beta(\alpha)$ is it possible to obtain a time independent value for ε_0, through cross calibration with WHISPER.

Our density reference was a large set of WHISPER electron density data during all magnetosheath and solar wind data intervals in 2001 and 2002, provided via the CAA. PEACE electron density moments were calculated using data from the LEEA sensors (to minimise the risk of count rate saturation which is greater for HEEA sensors) and applying α and β factor efficiency corrections and a preliminary value of ε_0. In the magnetosheath and solar wind, a LEEA sensor can capture the full particle distribution, so these are full rather than partial moments. In such environments the particle flux is large enough that ASPOC makes little difference to the spacecraft potential, so our sample was selected without reference to the ASPOC status. Figure 11 shows a quite narrow and tall histogram of ratios of PEACE/WHISPER densities, peaking near 0.8 for the particular case of Cluster 1 LEEA. The preliminary value of ε_0 was subsequently reduced so as to shift the peak to a value of 1. The new value of ε_0 is used in the updated calibration dataset.

For events where the HEEA sensor also fully covered the energy range occupied by these solar wind and magnetosheath plasmas, the HEEA ε_0 value was similarly adjusted to ensure agreement of HEEA, LEEA and WHISPER densities. There was no systematic attempt to filter out cases where γ_{ijk} is less than 1, but some cases where a problem was clearly apparent were removed. The process was repeated for all four spacecraft. This activity is now considered to have been completed.

Fig. 11. Illustration of the approach used to correct the ε_0 absolute detector efficiency parameter. PEACE LEEA densities are calculated using efficiency corrections related to detector gain variations (α and β), with a value for ε_0 produced during ground calibration. A comparison is then made with densities determined by WHISPER. The examples here are Cluster 1 data from magnetosheath and solar wind intervals in 2001 and 2002 (using CAA WHISPER data). The most frequently occurring ratio of PEACE LEEA to WHISPER densities, indicated by the histogram peak, shows the discrepancy associated with imperfect knowledge of ε_0 and can be used to determine the correct value of ε_0
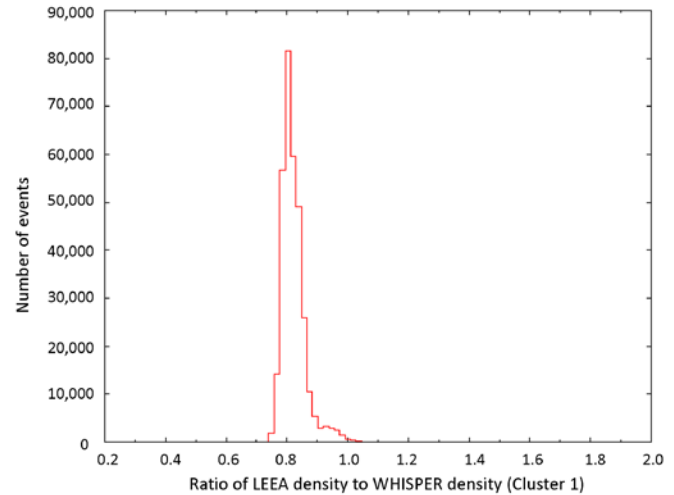
6.2 PEACE-WHISPER Cross-calibration: Verification of PEACE α correction factors

Figure 12 shows a comparison of electron density values determined by PEACE and by WHISPER, from a randomly selected magnetosheath interval, in which the plasma occupied the energy range below 1 keV. The data files were sourced from the CAA. The difference between the two datasets is typically less than 1 cm^{-3}, and the ratio between them shows agreement to within 5%. These results rely on the accuracy of the α (and β), and ε_0 calibration parameters, as well as a proper moments determination process taking account of spacecraft potential and eliminating spacecraft electrons.

There is an ongoing activity to seek useful test intervals in higher energy plasmas for which reliable density is available from WHISPER or WIDEBAND, but far fewer satisfactory intervals are available than for the magnetosheath, as the density tends to be too low for these instruments to give accurate results (e.g. see Masson et al., 2008). Although we have no reason to think that there is a problem at higher energies, density comparisons for cases with electron energies in the plasmasheet range would complete the in-flight validation of the calibration across the full PEACE instrument energy range.
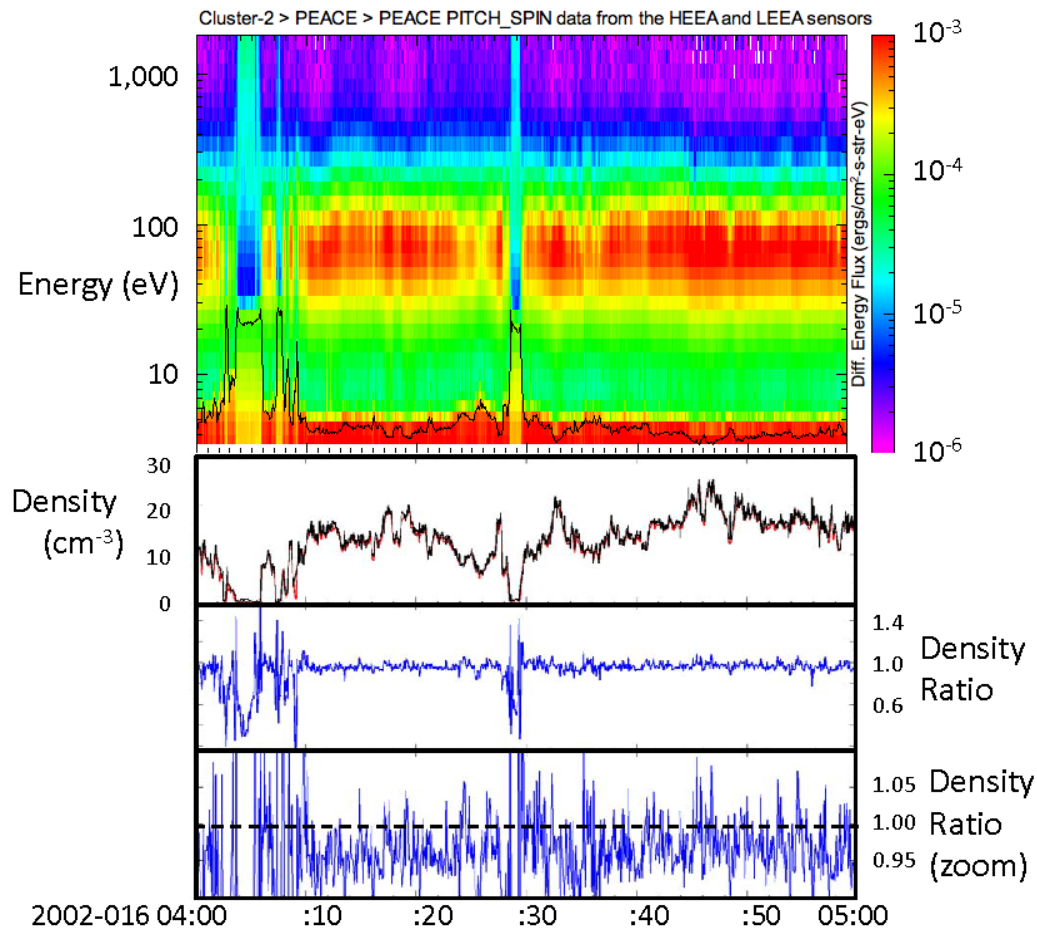
Fig. 12. Illustration of the accuracy of PEACE density moments for a 1 hour magnetosheath interval. The spectrogram confirms that the LEEA sensor measured the complete energy range occupied by the magnetosheath plasma. The black trace indicates the EFW probe-spacecraft potential energy, as a proxy for the slightly larger energy that is gained by an electron accelerated through the spacecraft potential, which must be allowed for in the density calculation. The next panel shows the PEACE and WHISPER densities (from CAA files) in red and black. The lower panels show that the ratio of these two time series is generally around 95%, sometimes closer to 100%. The intervals where the ratio departs significantly from 1 are periods of elevated spacecraft potential, and the WHISPER CAA file quality factor is rather low here, indicating less reliable density determination from the WHISPER wave data.

6.3 PEACE-EFW/FGM Cross-calibration: Verification of PEACE β correction factors

The $v\perp_z$ parameter determined by PEACE is expected be consistent with the electric field drift velocity determined using electric and magnetic field data from EFW and FGM. The electric field is only available in the spin plane, so it is only the spin axis component of $v_E = ExB/B^2$, derived from spin plane components of E and B, that is well determined by this method. These data are less re-

liable in cases of weak magnetic field, or magnetic field vector near the spin plane. Comparisons of $-vxB$ with individual components of E are also possible, but are not shown here.
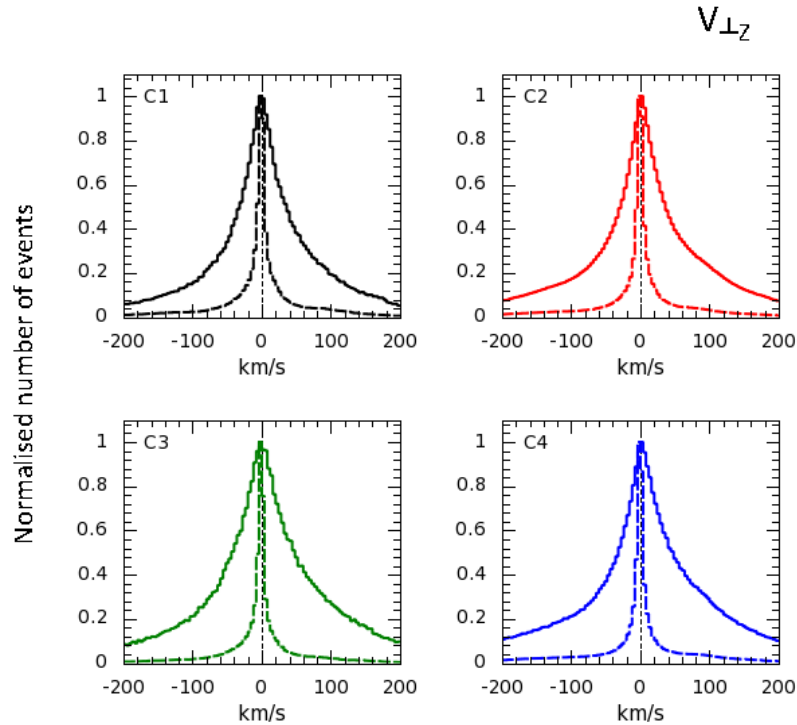

Fig. 13. Illustration of the difference between spin-axis component of $v\perp$, as determined by from ExB/B^2 and by PEACE, for magnetosheath and plasmasheet events in 2001. Note that in all cases the most commonly occurring value is 0 km/s, and that the electric field derived values show a very much narrower spread of values. A much larger number of electric field derived results are seen at small speeds, so the histograms were normalized to 1 to allow a clear comparison.

Figure 13 shows a set of electric field derived $v\perp_z$ values from 2001 provided by the CAA (only via the command line interface at the time of writing), which are available for all 4 spacecraft, together with the corresponding values from PEACE (using dual sensor moments). The dataset includes plasmasheet and magnetosheath intervals. The electric field derived values are also centered on 0 km/s, but show a much narrower spread, and when presented as an occurrence frequency histogram, a correspondingly taller peak; hence we show the two histograms together after normalization. Although the electric field derived values are often very good, it is worth recalling that the requirements on the magnetic field mean that the technique is not applicable in such a wide range of situations as those for which CIS and PEACE can measure bulk flow velocities. Also, occasionally, issues such as incorrect EFW bias currents, or cold ion wakes (or, usually less significantly, the electric field offset in the sun direction) may introduce errors which the user should be cautious about.

Figure 14 compares the two types of $v\perp_z$ measurements in a specific randomly selected interval. During this rather long interval, in which the spacecraft crosses from the magnetosheath to the polar cap via the cusp, the two measurements generally agree to within 30 km/s or better, i.e., to within 20% when significant (~100 km/s) flows are present.
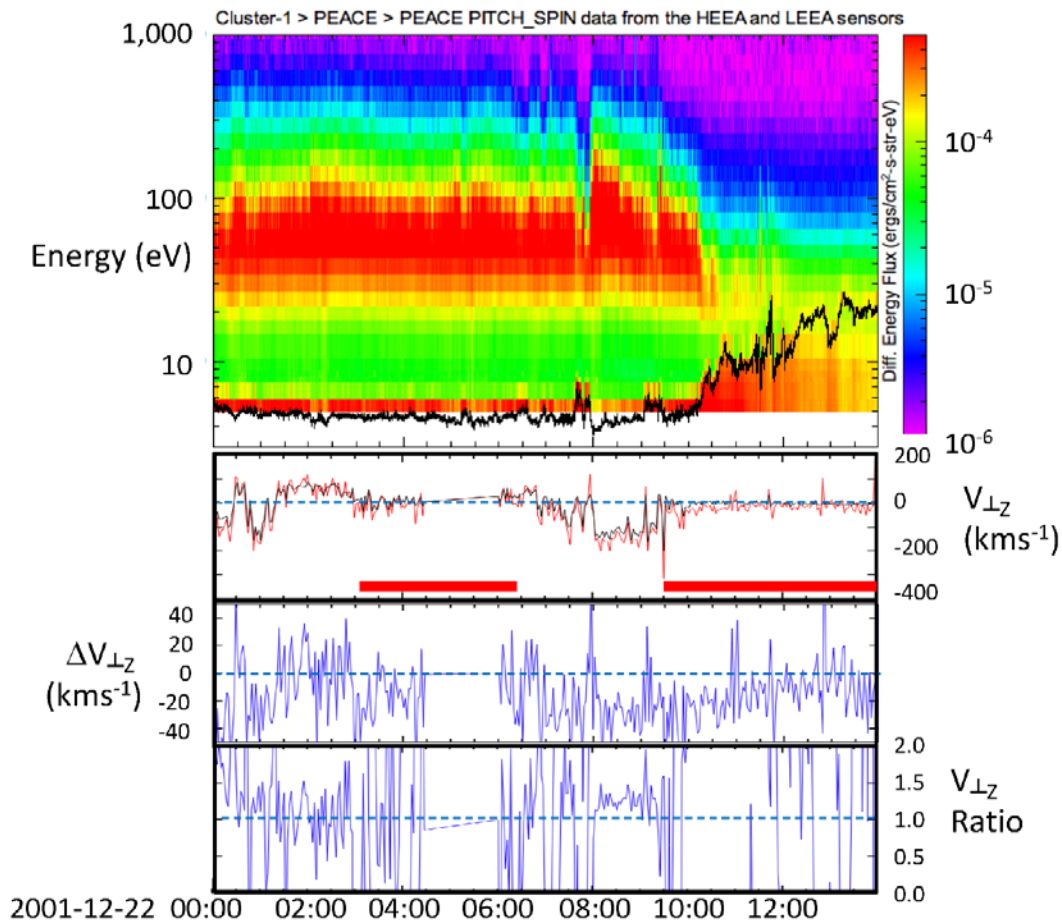

Fig. 14. Illustration of the accuracy of PEACE $v\perp_z$ moments for a 14 hour inbound pass beginning in the magnetosheath, passing through the southern high altitude cusp and entering the polar cap. The spectrogram confirms that the LEEA sensor measured the complete energy range occupied by the magnetosheath/cusp plasma. The black trace in the spectrogram indicates the EFW probe-spacecraft potential energy, as a proxy for the slightly larger energy that is gained by an electron accelerated through the spacecraft potential, which must be allowed for in the moments calculation. The next panel shows the $v\perp_z$ values from PEACE and from the *ExB* method (from CAA files) in red and black. The next panel shows the difference (PEACE – *ExB*) between them and the lowest panels show the ratio of these two time series (PEACE/*ExB*). The ratio is naturally rather large where the values are very small (intervals highlighted by red horizontal bars) but where there are significant flows we see ratios in the range $1 \pm \sim 0.2$. In all regions we see differences of order only 20-30 km/s.

6.4 PEACE-CIS Cross-calibration: Verification of PEACE β correction factors

A similar test can be carried out using ion velocity measurements from the CIS experiments, although not for all spacecraft. CIS is inoperative on C2 and does not provide reliable $v\perp_z$ on C3 except during the early part of the mission. The $v\perp_z$ parameter is used as a measure of the local convection speed of magnetic flux, which should be the same for ions and electrons that are all "frozen-in" to the local magnetic flux.

The CIS measurements have been calibrated by the CIS team, in a similar way to PEACE, prior to this comparison (see McFadden et al., 2007). The ion moments used were calculated using the CIS team "cl" software for CODIF on C1 and C4. This dataset was not checked to eliminate cases where perfect agreement is not expected, such as when the CIS or PEACE moments are calculated using incomplete coverage of the range of energies occupied by the plasma energy distribution.
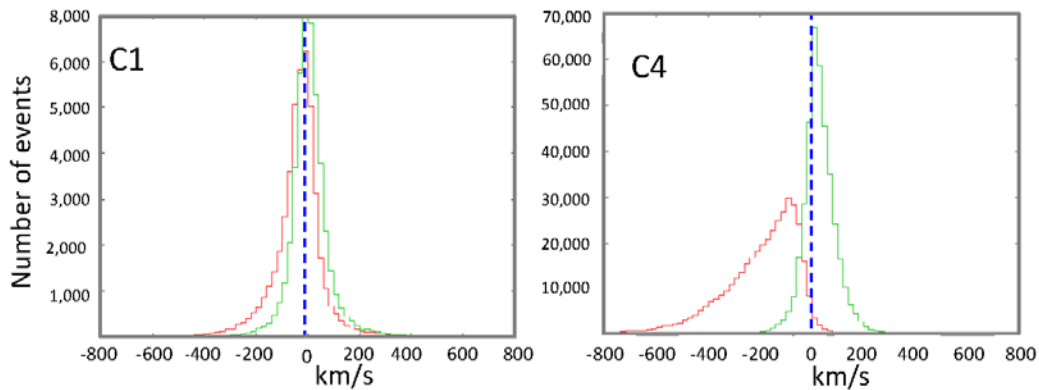

Fig. 15. Illustration of the difference $[v\perp_z]_{CODIF} - [v\perp_z]_{PEACE-HEEA}$, showing results for version 5.1 calibrations (green) and earlier version 4 calibrations (red). Note that the difference histogram shows a similar spread to the histograms of CODIF and HEEA data in Figures 4 and 5, suggesting that the spread is due to fluctuations which are un-correlated between PEACE and CIS.

Figure 15 shows residuals $[v\perp_z]_{CODIF} - [v\perp_z]_{PEACE}$ calculated for each of the 208 plasmasheet intervals, using (v5.1) and previous (v4) PEACE calibration datasets. The improvement in the PEACE results due to the v5.1 calibration is clear. The residuals histogram shows a similar spread to that of the CODIF histogram (Figure 9) and the PEACE histograms (Figure 10). This suggests that the $v\perp_z$ values are not correlated between the sensors, and that both represent a degree of random scatter about the "true" value of $v\perp_z$. If the measurements had all been "perfect" so that the histogram represented a range of conditions represented in the plasmasheet, the residuals would

have been zero, unless differential flows associated with electric current were present. On the other hand, this scenario is inconsistent with the narrow spread of values we see in the electric field based $v\perp_z$ (Figure 13).
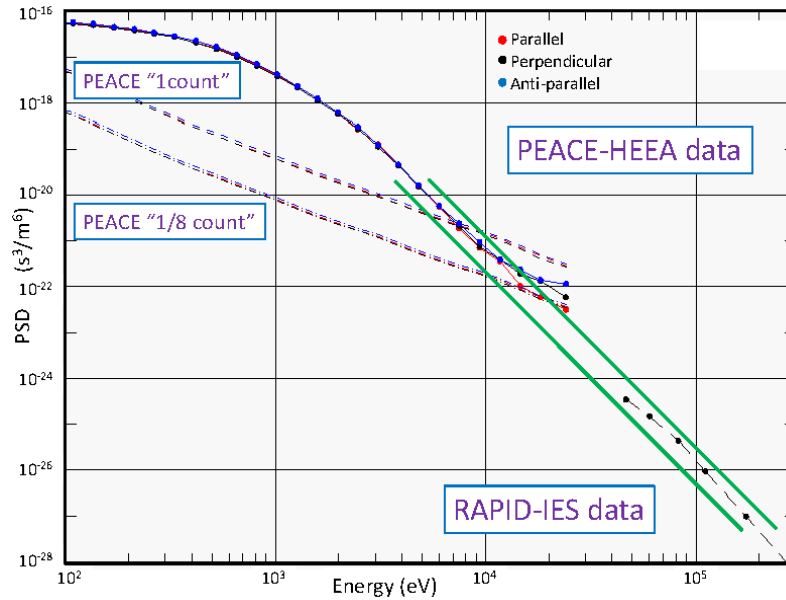

Fig. 16. Representative comparison plot showing electron phase space density vs energy measurements for three pitch angles from PEACE-HEEA and RAPID-IES on Cluster 2 on 10 September 2001, averaged over the interval 08:04-07 UT. There is an energy coverage gap intrinsic to the instrument designs. The trend in the PEACE data above 5 keV (indicated by parallel green lines) is quite well matched by the RAPID data above 50 keV. The plot also shows dashed lines which indicate the phase space density values corresponding to a hypothetical average background count level of 1 count per accumulation in PEACE data, and of a more realistic 1/8 count level background. In this case, the background magnetic field is aligned close to GSE X, so that the anode which measured the parallel (0°) pitch angle looks anti-sunward. The parallel trace clearly diverts from the data trend to follow the background curve at the highest PEACE energies. The traces for the other two pitch angles follow similar trends, but to show an expected slightly higher background associated with anodes facing sunward.

6.5 PEACE-RAPID-IES Cross-comparison

In order to investigate the inter-calibration of PEACE and RAPID-IES, some preliminary studies have been carried out, using comparison plots such as the example shown in Figure 16. The measurements made by IES were made at the same time as the PEACE measurements. We make the reasonable assumption that the same plasma population is being measured both the top of the PEACE energy range and in the IES range, so that the spectral gradient is expected to be the

same according to both instruments. The two parallel green guidelines in the figure show that a common gradient can be seen. The only PEACE points which do not follow the trend well are interpreted as being at energies where the signal falls below instrument background. The general conclusions are that the results based on the existing instrument calibrations, without any inter-calibration adjustments, are already quite good (although how good has not yet been quantified). It is clear from the figure that when making such comparisons one needs to be aware of the background count level in PEACE data since the plasma fluxes are often relatively low at the high energy end of the PEACE energy range. The studies have also shown that some care is needed in treating the low energy end of the IES energy range.
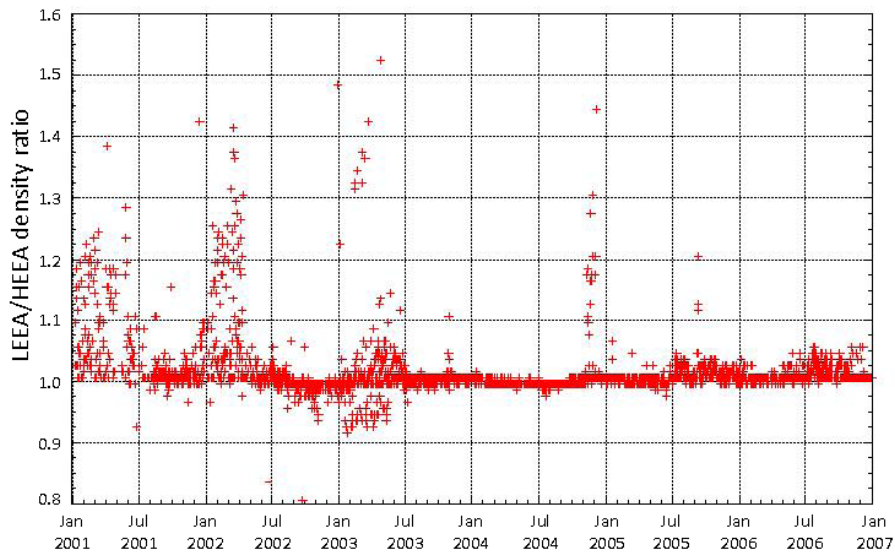

Fig. 17. The effectiveness of the HEEA/LEEA relative calibration is illustrated for Cluster-1 in this plot comparing densities n_L/n_H. For each case, the density is calculated using 3DR data transmitted to the ground, applying the v5.1 calibrations in use at CAA at the time of writing, and applying corrections for spacecraft potential and removal of spacecraft electrons. The density n_L is calculated using LEEA data in the energy overlap region while the density n_H uses HEEA data in the overlap region. Thus any difference between the two densities is expected to be due to differences in calibration of the energy overlap region. Generally the ratio is very satisfactory, and lies within 1 or 2% of a perfect result, though there are some exception. The most obvious exceptions are in the early months of 2001, 2002 and 2003, when the HEEA sensor was used in the magnetosheath. Some of the magnetosheath events had sufficiently high fluxes that the HEEA sensor saturated and returned too few counts, hence leading to a density underestimate and a ratio >1. These may be considered as examples of situations where $\gamma < 1$ (see 1.2.3). For this reason, the CAA Moments data product uses the LEEA data in the energy overlap region.

6.6 PEACE HEEA and LEEA sensor comparisons

To illustrate how well the overall calibration works, and how similar the results from the HEEA and LEEA sensors are, we present in Figure 17 the ratio n_L/n_H of densities measured in the same band of energies in the same plasma by LEEA and HEEA. The plot covers 6 years (compared to the 2 year interval used for determining ε_0) and shows that the inter-calibration is usually very good, with the ratio being 1 ± 0.02 for much of the time. The main exceptions are intervals in the spring of years 2001, 2002 and 2003 where the ratio is sometimes > 1, consistent with under-counting by HEEA in the high fluxes of the magnetosheath, i.e., cases when $\gamma_{ijk} < 1$. After 2003, the HEEA sensors were used less frequently in the solar wind and magnetosheath. At present, we simply flag time intervals in the PEACE CAA files where γ may depart from 1 and do not attempt a correction.

6.7 Four-spacecraft PEACE comparisons

Figures 18 and 19 illustrate good relative accuracy between the 4 Cluster PEACE instruments for randomly selected magnetosheath and plasmasheet burst mode intervals, using the CAA PEACE (version 1) dual sensor Moments data product. As in earlier figures, $v\perp$ is used to avoid differences that might arise if there are magnetic field-aligned beams at some spacecraft and not others. Exact agreement is not expected as the spacecraft are not perfectly co-located (~200 km apart in the magnetosheath case and ~4,000 km apart in the plasmasheet case). Nonetheless, values are generally very similar and the time series show the same trends between spacecraft. The CIS data (not shown) exhibit very similar behaviour, including the unusual variations in the y and z components of the magnetosheath flow in Figure 18 (probably related to solar wind current sheets transiting the magnetosheath) and the enhanced plasmasheet flows near 09:18 UT in Figure 19.
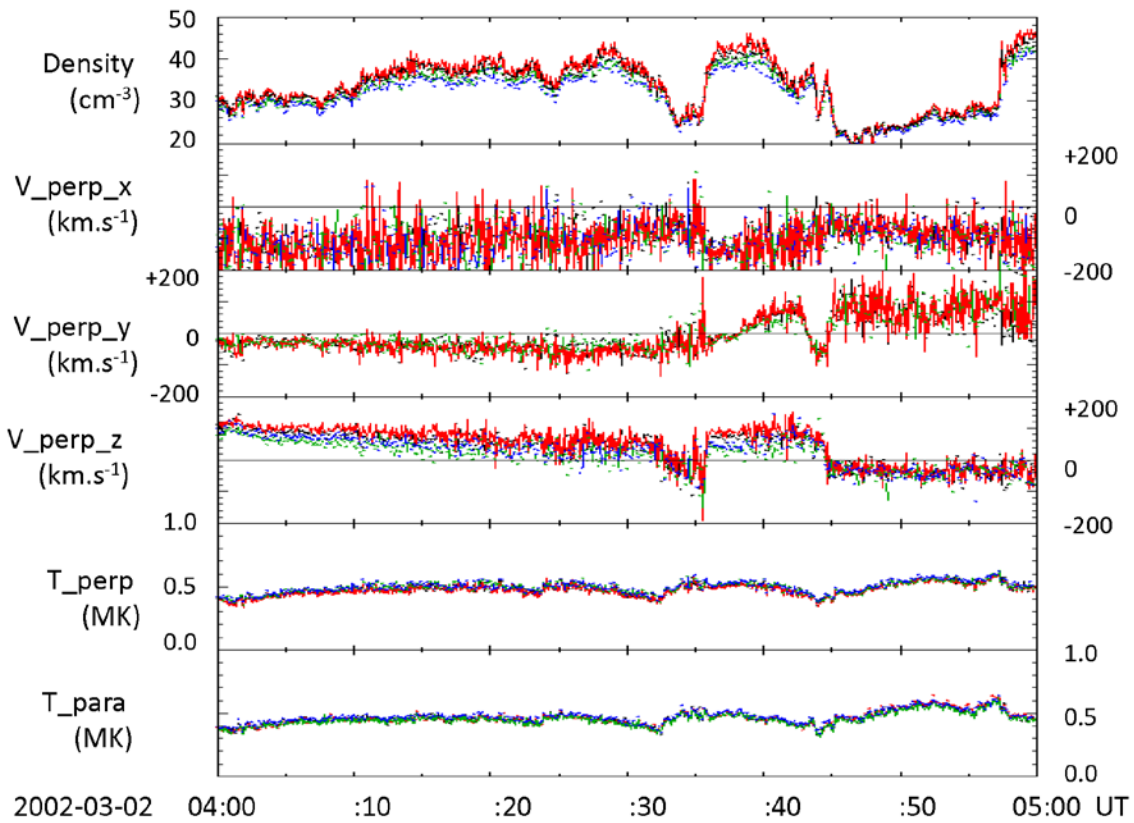
Fig. 18. Illustration of the relative accuracy of CAA PEACE Ver1 moments for randomly selected 1 hour burst mode (BM) telemetry intervals in the magnetosheath. Spacecraft separation is ~200 km. Data traces use the usual colour code: C1 black, C2 red, C3 green, C4 blue. Moments data from C1 and C3 is less frequent than spin rate, even though this is BM, as complete 3D distributions from both PEACE sensors are not available for each and every spin. Agreement is quite good in all parameters.

Fig. 19. Illustration of the relative accuracy of CAA PEACE Ver1 moments for randomly selected 1 hour burst mode (BM) telemetry intervals in the magnetotail plasmasheet. Spacecraft separation is ~4,000 km. Data traces use the usual colour code: C1 black, C2 red, C3 green, C4 blue. Moments data from C1 and C3 is less frequent than spin rate, even though this is BM, as complete 3D distributions from both PEACE sensors are not available for each and every spin. Agreement is quite good in all parameters.
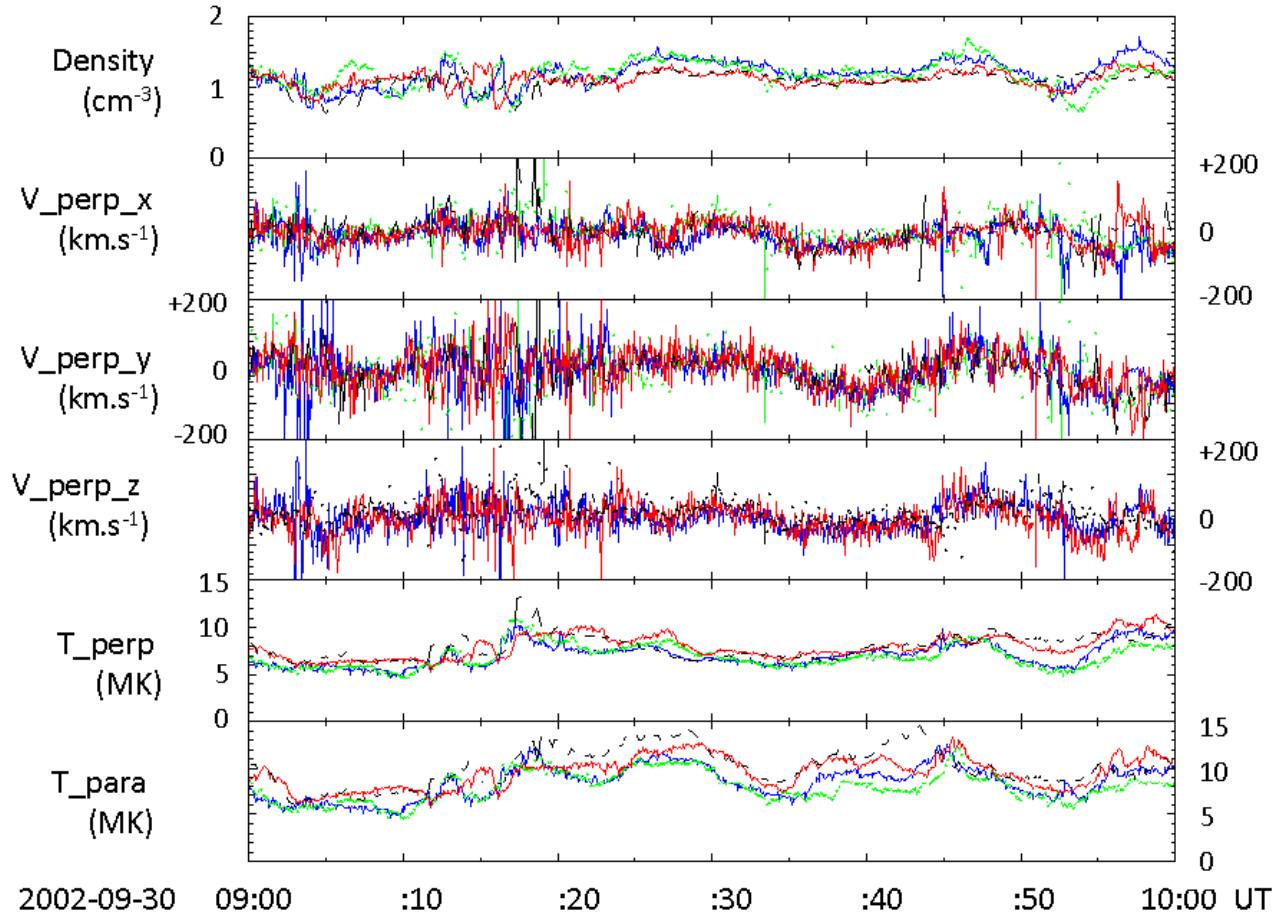
7 Summary

This report explains the internal PEACE team calibration work to monitor and correct for evolution of the MCP performance in each of the 8 sensors.

The absolute efficiency of each of the PEACE sensors was established by an in-flight cross-calibration activity using a reference electron density dataset provided to CAA by the WHISPER team. This work is now complete.

Similar work with the WHISPER and WIDEBAND teams continues as a continuing effort to verify our work (based on PEACE test data) to map detector sensitivity variation history for each PEACE sensor. In particular we will continue work in collaboration with the WHISPER team to track detector sensitivity of the sensors as our usual method has become inapplicable.

Comparisons of spin axis component of velocity with the ExB velocity derived from EFW/FGM data, and the spin axis velocity results of the CIS team also continue, to ensure that inter-anode calibration corrections for recently acquired data are as effectively calibrated as data from earlier in the mission.

Comparisons with electron data from RAPID_IES appear to be fairly satisfactory.

8 Acknowledgements

We thank ESA for funding CAA work, the CAA team for supporting cross-calibration activity as a priority within the CAA, and members of other PI teams who have helped us to carry out the work reported here.

9 References

Cully, C.M., R.E. Ergun and A.I. Eriksson, Electrostatic structure around spacecraft in tenuous plasmas, *J. Geophys. Res.*, 112, A09211, doi:10.1029/2007JA012269, 2007.

Doss, N, A.N. Fazakerley, B. Mihaljčić, A.D. Lahiff, R.J. Wilson, D. Kataria, I. Rozum, G. Watson and Y. Bogdanova, In-flight calibration of the Cluster PEACE sensors, Geosci. Instrum. Method. Data Syst., 3, 59-70, doi:10:5194/gi-3-59-2014, 2014

Fazakerley, A.N., A.D. Lahiff, R.J. Wilson, I. Rozum, C. Anekallu, M. West, H. Bacai, Cluster-PEACE In-flight Calibration Status, in *The Cluster Active Archive: Studying the Earth's Space Plasma Environment*, edited by H. Laakso. M. Taylor, C. P. Escoubet, pp.281-300, Springer, 2010a.

Fazakerley, A.N., A.D. Lahiff, R.J. Wilson, I. Rozum, C. Anekallu, M. West, H. Bacai, PEACE Data in the Cluster Active Archive, in *The Cluster Active Archive: Studying the Earth's Space Plasma Environment*, edited by H. Laakso. M. Taylor, C. P. Escoubet, pp.129-144, Springer, 2010b.

Fazakerley A.N, A.D. Lahiff, R.J. Wilson, M.G.G.T. Taylor, CAA Interface Control Document for PEA, CAA-PEA-ICD-0001, v5, 2008

Henderson, P. D., C. J. Owen, A. D. Lahiff, I.V. Alexeev, A. N. Fazakerley, L. Yin, A. P. Walsh, E. A. Lucek, and H. Reme, The relationship between jxB and div(Pe) in the magnetotail plasma sheet: Cluster observations., *J. Geophys. Res.*, 113, A07S31, doi:10.1029/2007JA012697, 2008.

Johnstone A.D., C. Alsop, S. Burge, P.J. Carter, A.J. Coates, A.J. Coker, A.N. Fazakerley, M. Grande, R.A. Gowen, C. Gurgiolo, B.K. Hancock, B. Narheim, A. Preece, P.H. Sheather, J.D. Winningham, and R.D. Woodliffe, Peace: A Plasma Electron and Current Experiment, Space Sci. Rev. 79, pp. 351-398, 1997.

Masson, A., M.G.G.T. Taylor, O. Santolik, A.D. Lahiff, A. Rochel, P. Escoubet, X. Vallieres, A.N. Fazakerley, A. Asnes and H. Laakso, Electron density estimation in the magnetotail: a multi-instruments approach, in *The Cluster Active Archive: Studying the Earth's Space Plasma Environment*, edited by H. Laakso. M. Taylor, C. P. Escoubet, pp.261-280, Springer, 2010.

McFadden et al., In-flight Instrument Calibration and Performance Verification, in *Calibration of Particle Instruments in Space Physics,* M. Wuest, D.S. Evans and R. von Steiger (Editors), ISSI Scientific Report SR-007, International Space Science Institute, 2007.

Appendix A: Calibration Parameters for PEACE

This material is based on Fazakerley et al. 2010a.

Introduction to the Calibration Parameters

Every spin, each PEACE sensor makes a series of measurements in different look directions and energies to sample all or part of the full velocity distribution of the plasma electrons. An individual measurement is intended to reveal the velocity space density of the electrons in a small region of velocity space, described in terms of a restricted energy (or equivalently speed) interval k and a direction defined by polar angle i and azimuth angle j, which is called f_{ijk}.

The relationship between measured quantities, calibration factors and f_{ijk} is given as follows:

$$f_{ijk} = P_{ijk} / (t_{acc} \, v_k^4 \, G_i \, \varepsilon_{ik})$$

where:
- t_{acc} is the data accumulation time, a fixed fraction of the spin period
- v_k is the mean value of the measured electron speed during time t_{acc}
- G_i is the geometric factor for the ith polar angle sector, which in a sufficiently concentric analyser, reduces to a single value G for all sectors
- P_{ijk} is the number of counted electrons after dead time correction (related to instrument electronics not the MCP), and
- $\varepsilon_{ik} = \varepsilon_0 \, \varepsilon(v_k^2)_i$ is the detector efficiency, which is expected to vary with position on the detector and with electron energy

Ground calibration work provides values for the energies (speeds) measured during energy sweeps, v_k, the geometric factor G_i and the relative sensitivity of the detector $\varepsilon(v_k^2)_i$, under conditions of optimum detector performance. These are used as the baseline from which any in-flight calibration corrections are made.

It is challenging to establish good values for absolute detector efficiency ε_0, during ground calibration, due to the difficulty of measuring the current in an electron beam in a calibration facility

with sufficient accuracy (i.e., in generating a beam with very well determined f_{ijk}). Furthermore, although the MCPs are kept purged with dry nitrogen as much as possible before flight, they are exposed to the atmosphere at least once between ground calibration and orbit (at the launch site) which may affect their performance.

Calibration Parameters: HEEA and LEEA

The HEEA and LEEA sensors are intended to be identical, except for having different geometric factors (G) due to a different mechanical design for the electrostatic analyser entrance (see Johnstone et al, 1997). All 8 sensors use the same equipment to control electron energy selection and to count detected electrons. Care was taken to make the electrostatic analysers of all the HEEAs as mutually identical as possible, and similarly for the LEEAs. The least controllable aspect of the design is the efficiency (ε_{ik}) of the individual micro-channel plate (MCP) detectors in each sensor. The calibration parameters mentioned above were measured in a test chamber to ensure that the individual sensors were well characterized and that their performance was identical to within specified tolerances before the instruments were accepted for flight.

Calibration Correction Factors

Three aspects of the instrument calibration were expected to vary during flight operations. The detector efficiency was expected to decline over time, and to require occasional correction by using increased voltage levels across the MCP.

The bulk velocity (determined by integration of f_{ijk} collected during each spin) was expected to possibly exhibit errors in the spin axis component due to errors in the determination of the relative sensitivity of the anodes; even small errors in inter-anode calibration could cause large errors in the bulk velocity measurement.

The detector sensitivity was also expected to respond by under-counting in sufficiently high flux environments, and ground tests of flight detectors suggested this could sometimes affect HEEA (though not usually LEEA) in the magnetosheath.

This scenario can be discussed in terms of additional factors in the expression for detector sensitivity, as follows

$$\varepsilon_{ik} = \alpha\varepsilon_0 \ \beta_{ik}\varepsilon(v_k{}^2)_i \ \gamma_{ijk}$$

where

- $\alpha(t)$ is a time dependent correction factor for ε_0, used to describe the effect of sub-optimal detector efficiency (equally for all anodes),
- β_{ik} represents corrections to $\varepsilon(v_k{}^2)_i$, the relative sensitivity of different parts of the detector, which may in principle vary with energy and
- γ_{ijk} represents possible under-counting due to detector saturation in high flux environments (not to be confused with electronic dead time, which sets in at higher count rates). This is kept equal to 1 for the time being.

These parameters (α, β, γ) were each equal to 1 in ground test conditions, when the MCP gain was well above 2×10^6 electrons and beam fluxes were not strong enough to cause detector saturation. In practice, we have found that the β_{ik} term shows dependence on the detector sensitivity, and thus a more elegant formulation of the problem might involve merging the α and β terms.

Relationship between Calibration Parameters and Moments

It can be shown that the plasma velocity (second order moment of $f(v)$) is independent of geometric factor and instrument sensitivity terms G α ε_0, but is dependent on the relative sensitivity of different parts of the detector, i.e, the terms β_{ik} $\varepsilon(v_k{}^2)_i$. Therefore, achieving plasma bulk flow vectors in agreement with independent measurements from other instruments is a good test of successful determination of the β_{ik} $\varepsilon(v_k{}^2)_i$ terms.

It can also be shown that the plasma density is inversely proportional to the G α ε_0 terms, as well as having a more complex dependence on β_{ik} $\varepsilon(v_k{}^2)_i$. Thus accurate densities from PEACE show that all calibration factors are well characterized, including time dependent detector efficiencies. Conversely, to isolate the correct value for ε_0 requires that α and β and all other calibration factors have been properly determined, that a reliable reference for the electron density is available and that proper moments calculations have been performed.

Appendix B: Calibration Progress for PEACE

B.1 PEACE-WHISPER Cross-calibration: Verification of PEACE α correction factors

As discussed in 6.2 above, we have adopted a procedure based on the assumption that the WHI experiment provides accurate electron density in the magnetosheath, in which we adjust our MCP sensitivity parameter to achieve agreement in density values determined from PEACE LEEA sensors, with results from WHISPER. This method has been applied for the period Nov 2004 through to June 2015. MCP performance during the magnetotail crossing season is estimated using interpolation. Comparisons of HEEA and LEEA density in the energy overlap region are used to extend the calibration improvements to the HEEA sensors.

It has become increasingly difficult to perform calibrations using this method due to lack of useable intervals (good sheath, good overlap between HEEA & LEEA). Therefore, as of June 2012, we routinely perform special calibration operations during normal modes and when possible during burst modes. For these special operations the sensors are put in the same energy range to maximize the overlap. We perform these operations in the sheath, that way we can also compare HEEA data with WHISPER.

Figures 20 & 21 show the relative MCP sensitivity time history for the four LEEA sensors (fig. 20) and the four HEEA sensors (fig. 21) inferred using this method (the basis for calibration v6.0) in red and that produced using weekly MCP tests (the basis for calibration v5.2) in black, for each sensor. For each calibration there are two lines. The upper line is the alpha factor for when the MCP is operated at the normal operational level. The lower line is the alpha factor for when the MCP was operated 1 or 2 voltage levels below the normal operational level usually in the sheath and wind. Green vertical lines show the commanded MCP voltage level changes, while thruster firings are shown as blue vertical lines.
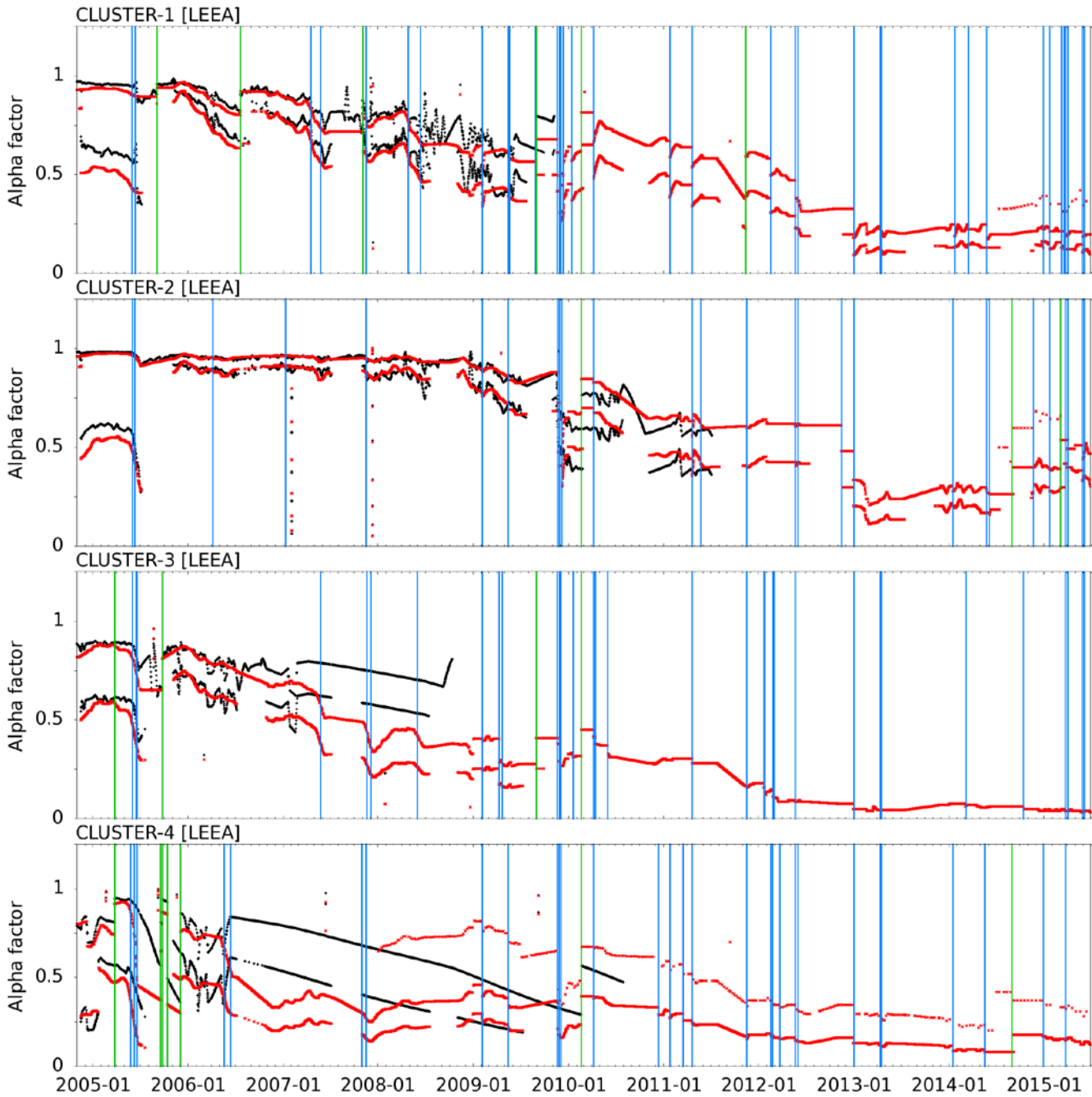
Figure 20: Alpha factor time history for the 4 LEEA sensors for period Jun 2005 to Jun 2015. Key: V6.0 alpha factors, V5.2 alpha factors, MCP operational level changes, Thruster firings

Doc. No.   CAA-EST-CR-PEA
Issue: 1.7
Date: 2017-05-10

Project: Cluster Active Archive   Page: 32 of 34

Figure 21: Alpha factor time history for the 4 HEEA sensors for period Jun 2005 to Jun 2015. Key: V6.0 alpha factors, V5.2 alpha factors, MCP operational level changes, Thruster firings
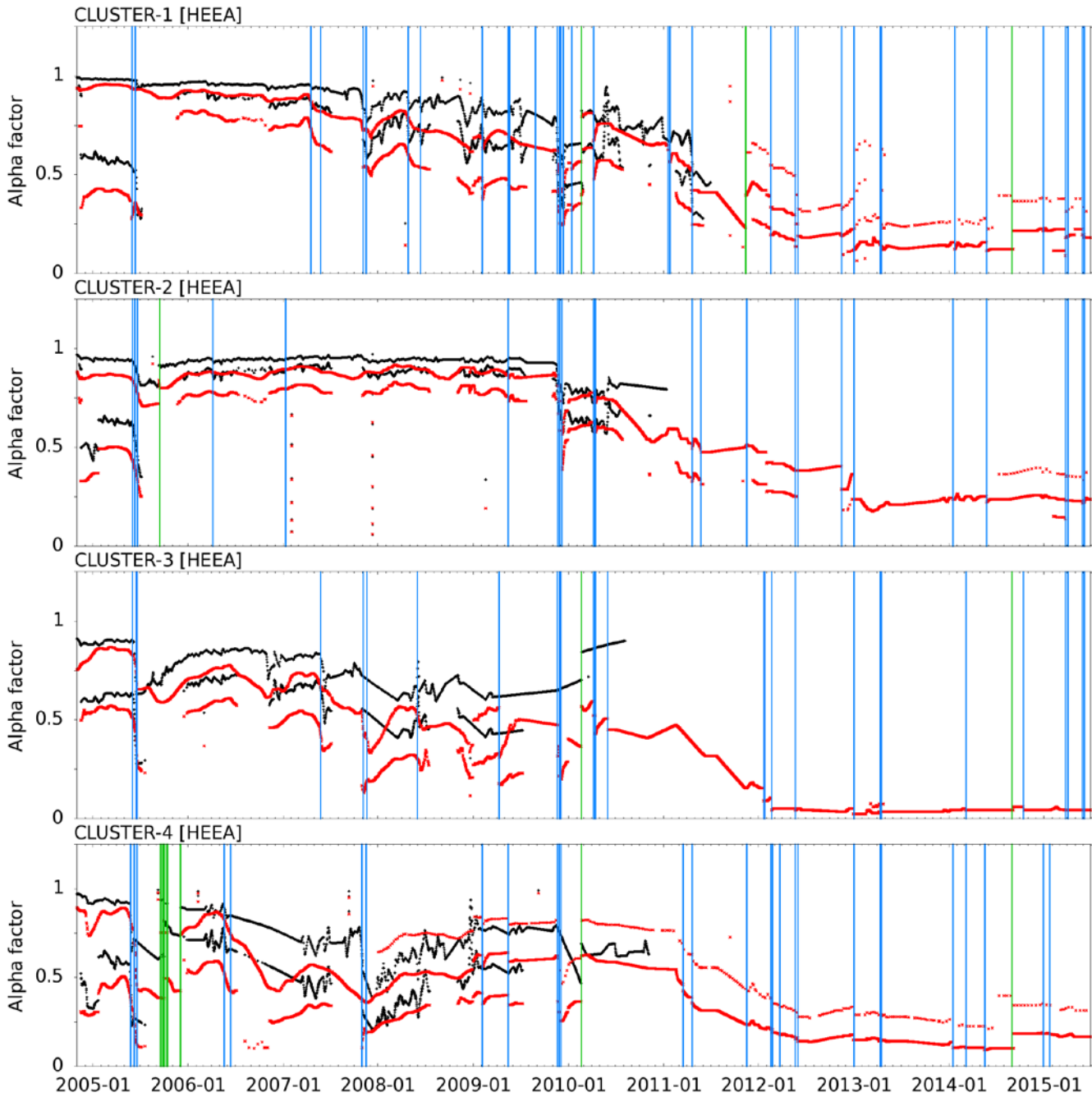
B.2 Determination of PEACE β correction factors

The knowledge of how inter-anode relative sensitivity differences change as a function of energy and gain is determined by the method outlined in section 5.2. The priority is to produce relative calibrations for pairs of anodes, in order to support improved quality moments calculations using 3DR data, so the analysis is based on 3DR and 3DXP data. In particular, there is no inter-anode calibration correction applied (so far) to datasets using all 12 anodes.

This type of calibration was done for the first ~6 years of the mission initially (e.g. see Table 1). Recent Inter-Anode calibration studies have been done for Years 2012 -2014, although data in the CSA has not yet been updated to reflect this work. Figure 22 illustrates ongoing work.
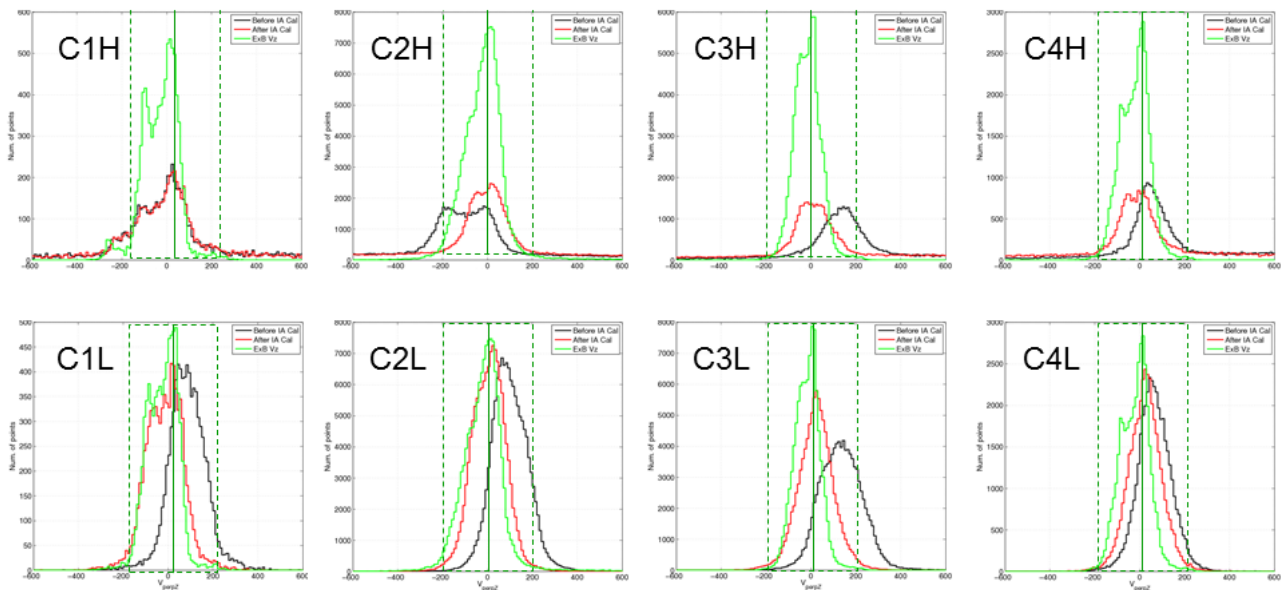

Figure 22: Distribution of z component of V⊥ for magnetosheath intervals in 2012; black is without inter-anode calibration, red is with inter-anode calibration and for comparison green is the same parameter derived from EFW and FGM data (similar to Fig 13). The effectiveness of the inter-anode calibration correction is clear.

Two instruments have an individual broken anode. For C2 LEEA (anode 2 of 12) this applies is from 15th May 2011 and for C3 HEEA (anode 3 of 12) this is from 22nd Aug 2005. For C3 HEEA, linear interpolation across the affected anode pair appears to enable quite effective correction, however the approach of doubling the counts in the end anode-pair for C2 LEEA is less effective and further efforts to improve the quality of the correction for this sensor are planned.

Appendix C: EFW potential correction to support PEACE calibration work

Typically, the overplotted probe-spacecraft potential from EFW tracks the variation in true spacecraft potential, as indicated by the boundary of the photoelectron population on a PEACE energy–time spectrogram, allowing for the effects of a probe-plasma contact potential (e.g. see Figures 12 and 14). Accurate knowledge of the spacecraft potential is required for good quality PEACE moments calculations in environments with significant electron fluxes at low energies.

EFW probe-spacecraft potentials have been consistently smaller on C3 than for C4 since at least 2005. Dramatic differences have been seen between C2 and C1 since ~ 21 April 2011 when the C2 spacecraft experienced atomic oxygen fluxes during particularly low altitude perigees passes.

The PEACE team has generated empirical corrections to the EFW potential data for use in alpha factor calibration work and in generation of PEACE Moments data for delivery to CSA. Thus far, these "corrected" potential data for C2 and C3 are not currently available from CSA.

Figure 23. Jul 2015 – Apr 2016 EFW potential corrections. Left hand column shows uncorrected C2 and C3 potential data compared to C1 and C4 potential data, for times when the pairs of spacecraft were in the same plasma environment. Corrections are based on linear fitting, quadratic fitting and in some cases a combination of both, for potentials above and below 10 V, typically on two monthly data intervals.